Bulk Mineralogy of Pleistocene Mediterranean Outflow Water Contourites at IODP Site 1387

Undergraduate Research Thesis
Presented in Partial Fulfillment of the Requirements
for graduation "with Research Distinction in Earth Sciences"
in the undergraduate colleges of
The Ohio State University

By
Amber Huston
The Ohio State University
20l5

Approved by

_____

Lawrence A. Krissek, Advisor
School of Earth Sciences

Abstract

Expedition 339 of the Integrated Ocean Drilling Program collected ocean sediment cores at seven localities in the Gulf of Cadiz and on the West Iberian margin, a contourite deposition system (CDS) influenced by the Mediterranean Outflow Water (MOW). The cores provide an insight into circulation and climate patterns at the time of sediment deposition, and the rapid sedimentation rate from MOW allows for a detailed look at this sedimentary record. Sediment at Site U1387 is Pleistocene in age, as calculated by a shipboard age/depth model, and bulk mineralogy has been analyzed on the portion of core 256-280 meters below seafloor, representing sediment deposition 1.014-1.236 million years ago. Samples were powdered and x-ray diffraction patterns were acquired from the randomly oriented grains. Relative intensity ratios of a distinctive diffraction peak for each mineral phase compared to quartz were used as semi-quantitative indicators of mineral abundance. Changes in these ratios over time were examined 1) to define covarying mineral assemblages and 2) to identify any consistent compositional changes during glacial/interglacial cycles. Quartz and dolomite relative abundances covary, and illite and 7Å clays covary, but calcite does not covary with any other minerals. No definite correlation to glacial/interglacial cycles could be made, but the covariation of minerals is hypothesized to be a result of changes in grain size. Quartz and dolomite indicate the presence of larger grain size, while illite and the 7Å clays indicate smaller grain size.

Table of Contents

Acknowledgements

First and foremost I would like to thank Dr. Larry Krissek for being a superb advisor and brilliant storyteller. Equally huge thanks to Dr. Anne Carey for being an inspiration and always keeping us undergrads on track, and to Dr. Matt Saltzman for getting me started with research at Ohio State and always being willing to help out. Much gratitude to Julie Sheets for patiently teaching me all about XRD and trusting me with her very expensive equipment. Good vibes to Erin Lathrop, my unofficial 2nd advisor, for teaching me lab techniques and putting everything in terms that a barista can understand. I cannot fully express my gratitude for the daily emotional support from Mackenzie Scharenberg, my more beautiful geotwin; Connor Gallagher, my SES husband; and Alex Rytel, a gentleman and a scholar and a dear friend. Thank you to my parents for even making my existence and college career possible, and thank you to my muse, Martyna, for being my muse, and Lindsay, for always knowing what to say. Sincere appreciation to Sleater-Kinney for creating magical music that both empowers me and embodies my everyday angst, and to Bill Murray for his perfect portrayal in *The Life Aquatic with Steve Zissou* of the sort of oceanographer I strive not to be. And lastly, my project would not be possible without the funding from the US Science Support Program to execute the International Ocean Discovery Program.

Introduction

The Integrated Ocean Drilling Program (IODP), now the International Ocean Discovery Program (still IODP), is an international effort to gain a better understanding of the Earth's oceans and their conditions in the past through drilling of ocean sediments and rocks. Expedition 339 (November 2011-January 2012) drilled two sites off the West Iberian margin and five sites in the Gulf of Cadiz, including Site U1387, which is examined here. The Gulf of Cadiz is a region of interest because of the influence of the Mediterranean Outflow Waters (MOW) and presence of associated contourite deposits. Figure 1 shows the location of U1387 and the other sites investigated during Expedition 339 (Expedition 339 Scientists, 2012a).

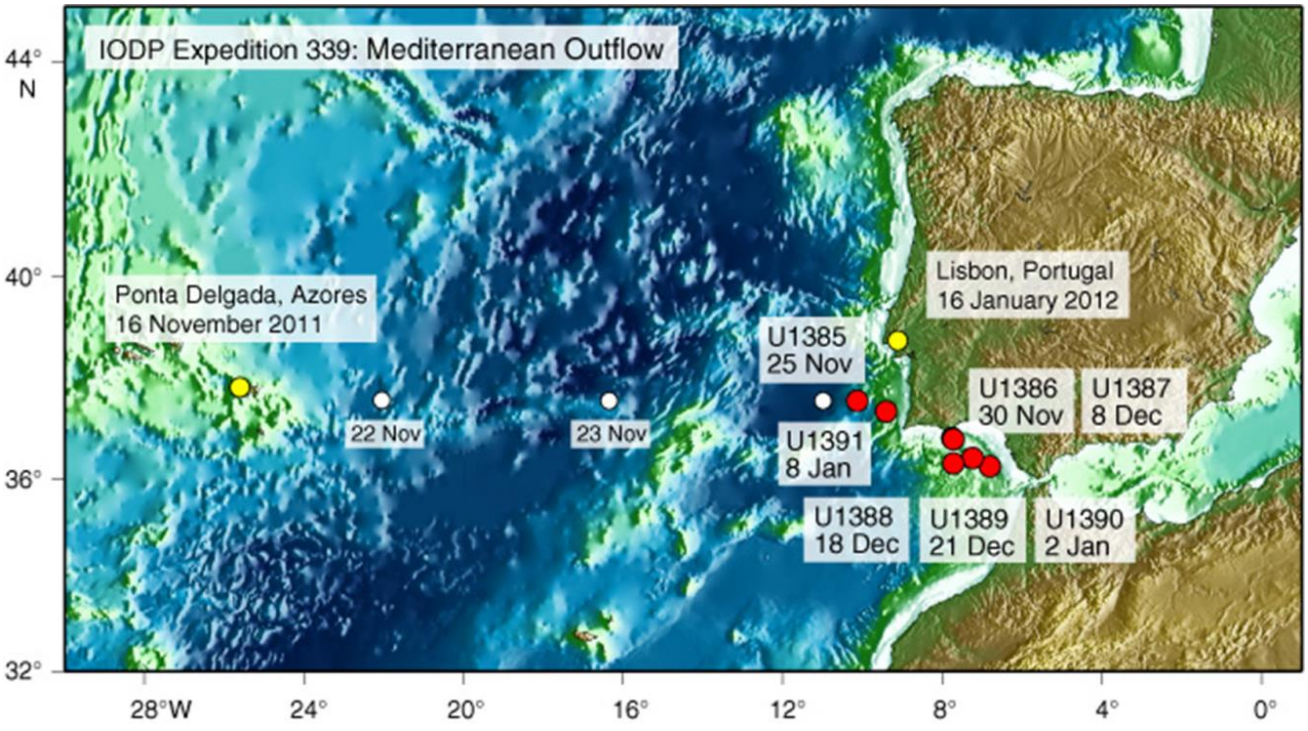

Figure 1: Expedition 339 Drilled Sites (Expedition 339 Scientists, 2012a)

MOW consists of the water exiting the Mediterranean Sea via the Strait of Gibraltar. This outflow has been occurring since the Strait opened during the late Miocene, and has greatly affected the evolution of the Gulf of Cadiz, as well as the Alboran Sea and the North Atlantic Ocean. The Faro Drift region is one example of its influence. As opposed to down-slope sedimentary processes such as turbidity currents, this region is dominated by along-slope processes, specifically contour-following currents and their deposits, contourites. After MOW passes through the Strait of Gibraltar and enters the Gulf of Cadiz, the current veers northwest as a result of the Coriolis effect. This results in the currents following along the bathymetric contours, with sediment deposited likewise (Hernández-Molina et al., 2014).

As with all coastlines, the Gulf of Cadiz is sensitive to sea level change, including changes caused by glacial/interglacial cycles. For example, when there is a sea level rise, as a result of the melting of ice during an interglacial, the core of the MOW current also rises. The "core" of a current is simply the section with the highest velocity. Because Site U1387 is located relatively close to the coast, the core of the MOW current is at this region during times of higher sea level, and is below it during lower sea level. Figure 2 shows each drilled site in relation to the direction of currents and the location of the upper and lower flows, as well as tectonic features (Hernández-Molina et al., 2006).

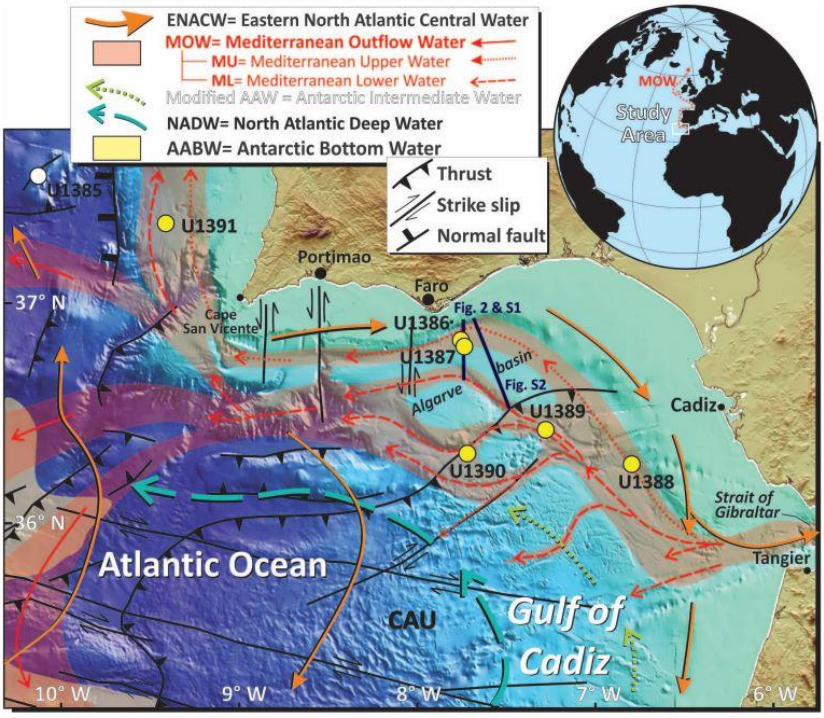

Figure 2: MOW Currents (Hernández-Molina et al., 2006).

Goals and Objectives

The overall goal of IODP Expedition 339 was to recover sediment from the Gulf of Cadiz that was deposited from the Miocene to the present, to include the period of the onset of MOW and its evolution over time. As mentioned above, MOW has since then had a great impact on the Alboran Sea, the North Atlantic Ocean, and the Gulf of Cadiz, so proxies carried by these sediments can give insight to changes in currents and climate.

In this study, the bulk mineralogy of a Pleistocene section spanning 1.014-1.236 mya is examined, with the intention of examining mineral abundance changes over time in relation to glacial/interglacial cycles.

Methods

Sample Collection

Three holes were drilled in December of 2011 at Site U1387 during IODP Expedition 339 of the JOIDES Resolution using the three standard coring systems: advanced piston corer (APC), extended core barrel (XCB), and rotary core barrel (RCB). Hole U1387A was drilled to 352.4 meters below seafloor (mbsf), Hole U1387B was drilled 338.3 mbsf, and Hole U1387C was drilled to 870 mbsf, the target depth. A total of 1270.7m was drilled, with 1084.95m of sediment recovered (Expedition 339 Scientists, 2012b).

The overlapping sections of the three holes were correlated using shipboard magnetic susceptibility and natural gamma-ray data and were assigned a composite depth along with the depth below seafloor. Ages were determined using paleomagnetic and biostratigraphic datums, and sedimentation rates for specific intervals of core were calculated.

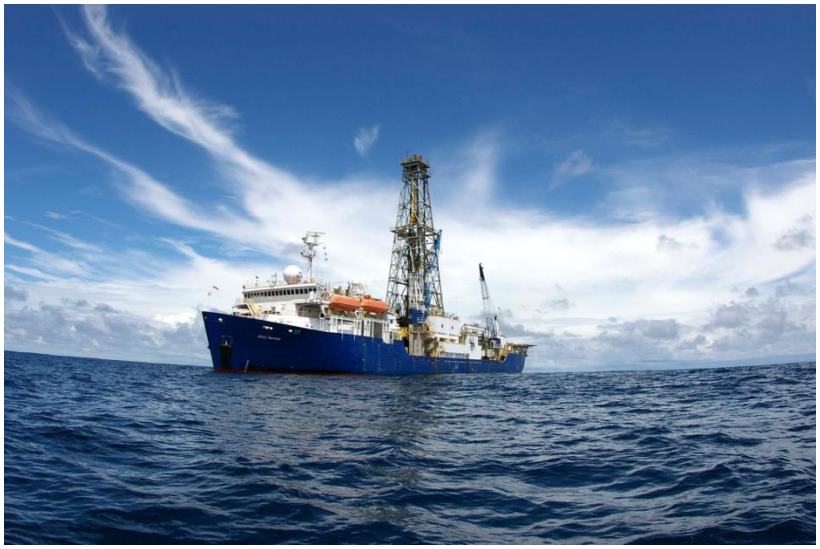

Figure 3: The JOIDES Resolution

Sample Analysis

For this study, 25 samples were analyzed. They span 279.99-341.31 meters composite depth (mcd), meaning they were collected approximately every 1.5 mcd. Because these samples were chosen along the composite section (the "splice"), the sample set includes materials from all three holes at Site U1387.

Individual samples were pulverized with a mortar and pestle. Samples were then back-loaded into a zero diffraction plate, as randomly oriented grains. X-ray diffraction patterns were collected using the PANalytical X'Pert Pro XRD in the Subsurface Energy Materials Characterization & Analysis Laboratory (SEMCAL) in the School of Earth Sciences at Ohio State University. A 1° divergence slit, 2° incident antiscatter slit, and 5.5° diffracted anti-scatter slit, and a brass mask were used, with no receiving slit. The step size was 0.020°2θ from 4.0-70.0° at 10s/step, with a voltage of 45 kV and a current of 20 mA.

Five replicates (20% of samples) were run to check for consistency in data collection and analysis.

Data Analysis

Diffraction patterns were analyzed in HighScore Plus. Background noise was determined by adjusting granularity and bending factor. Then a Peak Search was run to identify all prominent peaks in the pattern, and the Search and Match function was used to identify mineral phases that matched with each peak.

Quartz, calcite, dolomite, illite, and 7Å clays were found to be present in each sample, with their most diagnostic peaks being 4.25Å, 3.03Å, 2.88Å, 9.96-10.78Å, and

7.05-7.13Å, respectively. Areas under these peaks were calculated on HighScore Plus for quartz, calcite, and dolomite, and were calculated using Data Viewer for illite and the 7Å clays. Semi-quantitative abundance measures were calculated for each mineral by dividing its diagnostic peak area by the area of the quartz peak in the same sample. These intensity ratios cannot be related to used as absolute abundances, but can be used to identify relative abundance changes through time.

Each sample was assigned an age based on its particular depth at Site U1387 and the sedimentation rate determined from shipboard measurements (Expedition 339 Scientists, 2012a). This sedimentation rate was a constant 27.625 cm/ky through the depth interval considered here. To calculate each sample's age, its depth in mcd was divided by the sedimentation rate: age=mcd/(2.7625*10^-4 m/y). The sample ages were then compared to known ages of glacial/interglacial stage boundaries, taken from the Lisiecki-Raymo Marine Isotope Stage (MIS) stack (Table 1; Lisiecki and Raymo, 2005). The even numbered stages are glacials, while odd numbers are interglacials.

Table 1: Lisiecki-Raymo MIS Boundaries

Boundary	Age (ma)
28/29	1.014
29/30	1.031
30/31	1.062
31/32	1.081
32/33	1.104
33/34	1.114
34/35	1.141
35/36	1.190
36/37	1.215
37/38	1.244

Results

The mineral phases found to be abundant were quartz, dolomite, calcite, illite, halite, and interstratified clays. The clays with a diffraction peak at 7Å are interpreted as chlorite, kaolinite, and/or smectite, but are indistinguishable with the XRD technology used in this study and are grouped together. The areas under the diagnostic peaks for each mineral are listed in Table 2. The ratios of the minerals to quartz can be seen in Table 3. Figures 4-8 show the peak intensity ratio for each mineral through time and include the Lisiecki-Raymo glacial/interglacial stage boundaries.

Figures 4 and 5 show similarities in the change in abundance of quartz and dolomite through time, such the sharp increase at 1.06 Ma. Figures 6 and 7 show similarities in the change in abundance of illite and the 7Å clays, such as the sharp increase at 1.165 Ma . Calcite shows much less variation over time and does not trend with other minerals. There are peaks of mineral abundances during both glacials and interglacials.

Table 4 shows the percentage error for each mineral/quartz ratio based on comparison between original runs and replicates.

Table 2: Mineral Peak Areas

Composite Depth (m)	Age (ma)	Quartz	Calcite	Dolomite	Illite	7Å Clays	Halite
279.99	1.014	570.87	1292.14	370.56	127.1	202.5	128.57
284	1.028	576.12	1955.2	276.69	117.6	149.5	78
285.31	1.033	586.61	1453.4	422.2	136	52.7	195.29
288.06	1.043	523.43	1552.17	202.06	97.5	81	52.11
289.85	1.049	470.3	1589.75	312.2	107.9	77.1	28.93
292.71	1.06	677.75	1719.72	1115.82	95.3	106.1	
295.09	1.068	420.33	1627.29	297.66	74.3	56.8	60.36
298.09	1.079	557.19	2044.23	240.34	114.1	80.5	49.17
299.41	1.084	387.09	1667.99	79.8	84.2	50.7	64.04
303.09	1.097	523.74	1731.1	223.3	130.5	204.4	0.71
306.45	1.109	462.23	1811.55	315.09	139.3	129.6	107.8
309.8	1.121	431.89	1694.43	338.34	202.1	204.3	
311.51	1.128	614.2	1341.52	320.72	248.1	118.4	132.96
315.81	1.143	529.5	2014.53	383.61	161.5	108.9	101.22
317.6	1.15	619.94	1648.28	447.63	174.9	107.4	53.94
320.8	1.161	374.75	1848.08	339.24	150.7	113.9	
321.95	1.165	463.81	1446.09	317.56	310.9	236.4	76.97
327.23	1.185	451.17	1953.19	206.17	96.6	65.2	59.23
331.17	1.199	523.18	1743.1	201.51	95.1	100.8	33.25
332.75	1.205	522.06	1991.55	306.41	90	90.5	26.76
334.61	1.211	433.9	1686.84	187.74	155	159.4	
336.61	1.218	422.46	1564.58	103.52	110	99.7	
338.26	1.224	505.94	1841.73	156.97	105.3	169.8	79.5
341.17	1.235	493.73	1788.51	440.51	115.5	109.8	
341.31	1.236	507.1	1830.45	575.42	148.8	191.5	

Table 3: Mineral/Quartz Ratios

Composite Depth (m)	Age (ma)	Calcite/Quartz	Dolomite/Quartz	Illite/Quartz	7Å Clays/Quartz
279.99	1.014	2.26	0.65	0.22	0.35
284	1.028	3.39	0.48	0.2	0.26
285.31	1.033	2.48	0.72	0.23	0.09
288.06	1.043	2.97	0.39	0.19	0.15
289.85	1.049	3.38	0.66	0.23	0.16
292.71	1.06	2.54	1.65	0.14	0.16
295.09	1.068	3.87	0.71	0.18	0.14
298.09	1.079	3.67	0.43	0.2	0.14
299.41	1.084	4.31	0.21	0.22	0.13
303.09	1.097	3.31	0.43	0.25	0.39
306.45	1.109	3.92	0.68	0.3	0.28
309.8	1.121	3.92	0.78	0.47	0.47
311.51	1.128	2.18	0.52	0.4	0.19
315.81	1.143	3.8	0.72	0.31	0.21
317.6	1.15	2.66	0.72	0.28	0.17
320.8	1.161	4.93	0.91	0.4	0.3
321.95	1.165	3.12	0.68	0.67	0.51
327.23	1.185	4.33	0.46	0.21	0.14
331.17	1.199	3.33	0.39	0.18	0.19
332.75	1.205	3.81	0.59	0.17	0.17
334.61	1.211	3.89	0.43	0.36	0.37
336.61	1.218	3.7	0.25	0.26	0.24
338.26	1.224	3.64	0.31	0.21	0.34
341.17	1.235	3.62	0.89	0.23	0.22
341.31	1.236	3.61	1.13	0.29	0.38

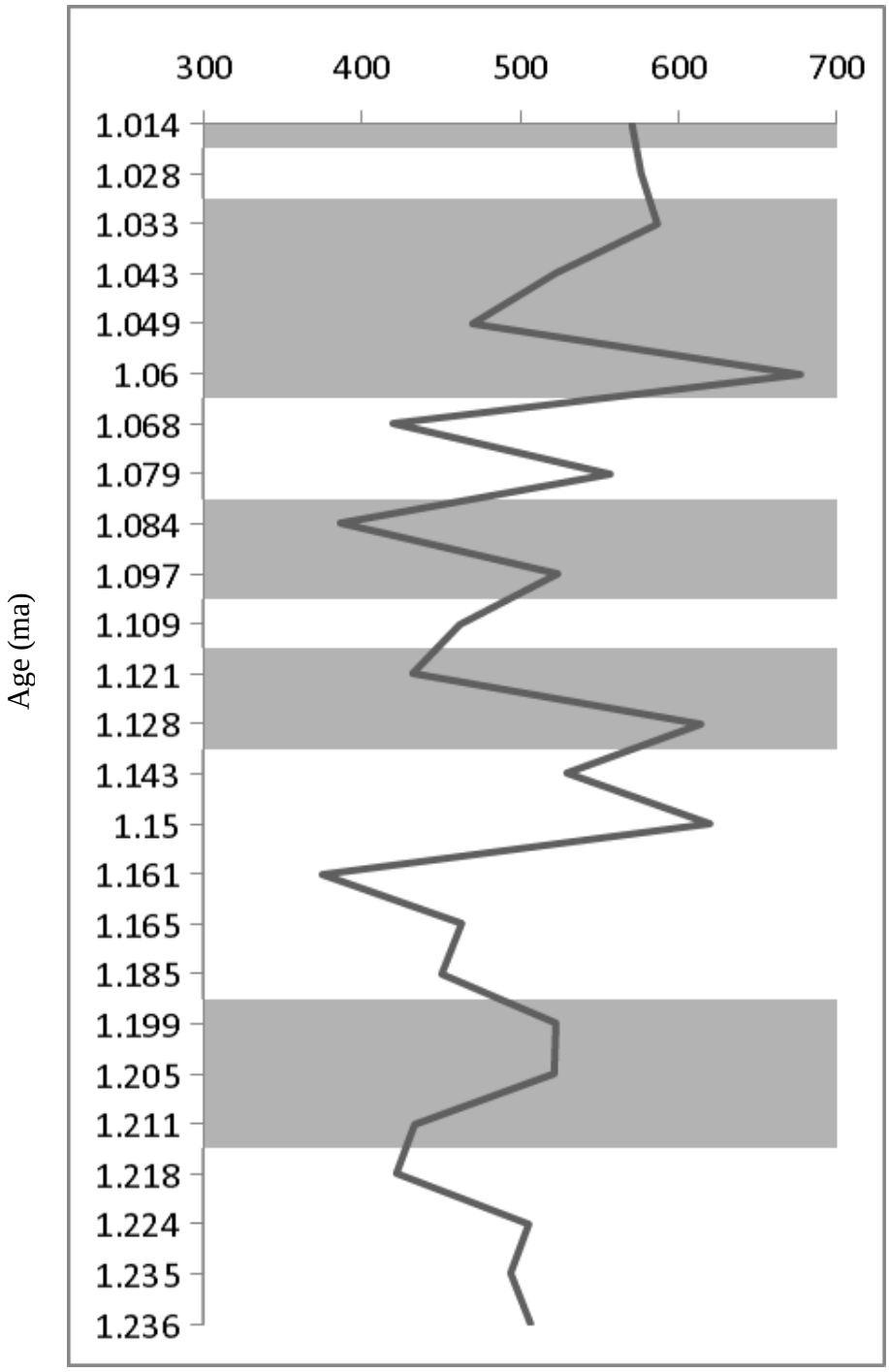

Figure 4: Quartz Intensity. Grey bands indicate glacials, white bands indicate interglacials.

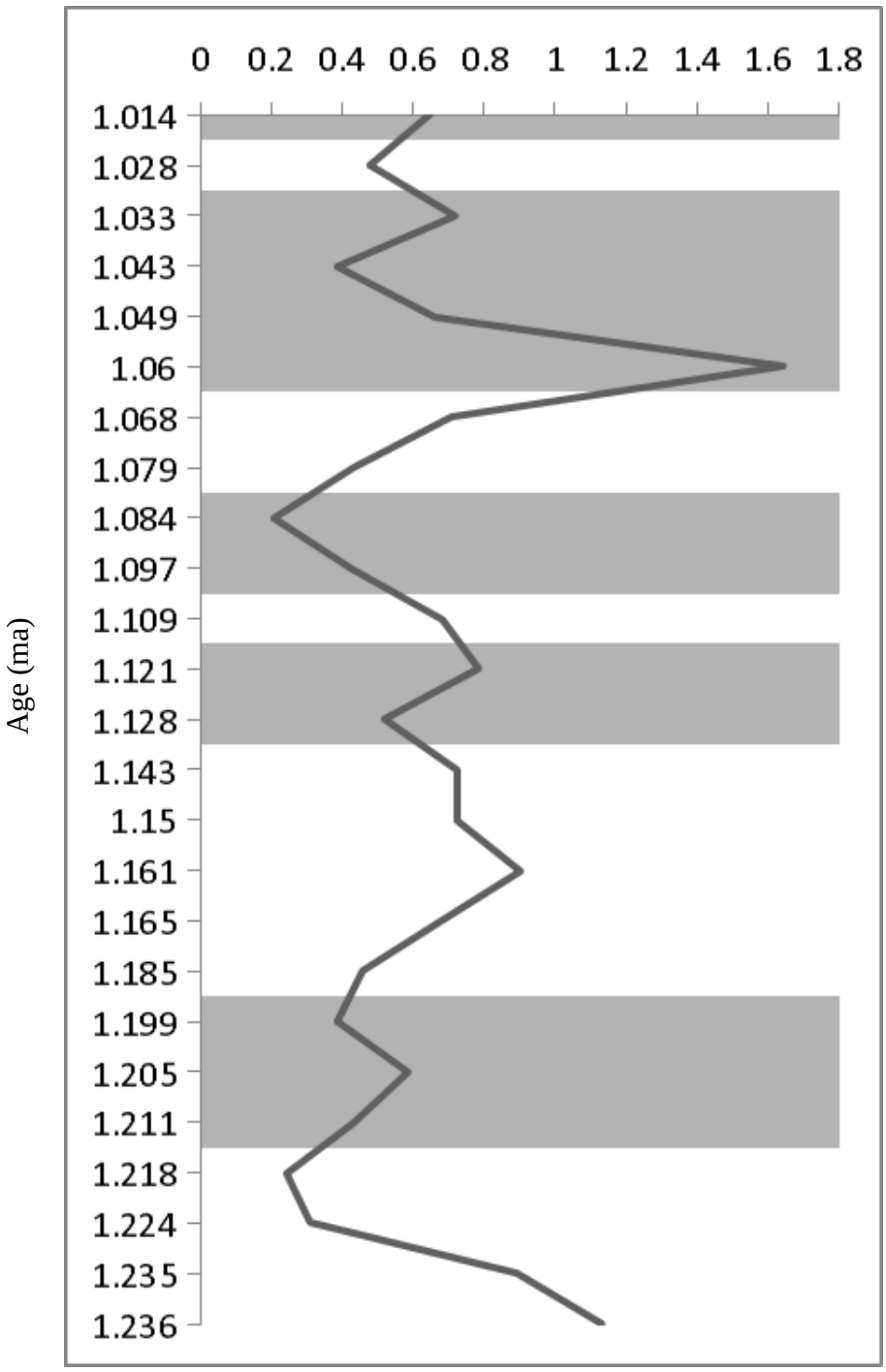

Figure 4: Dolomite/Quartz Intensity Ratio. Grey bands indicate glacials, white bands indicate interglacials.

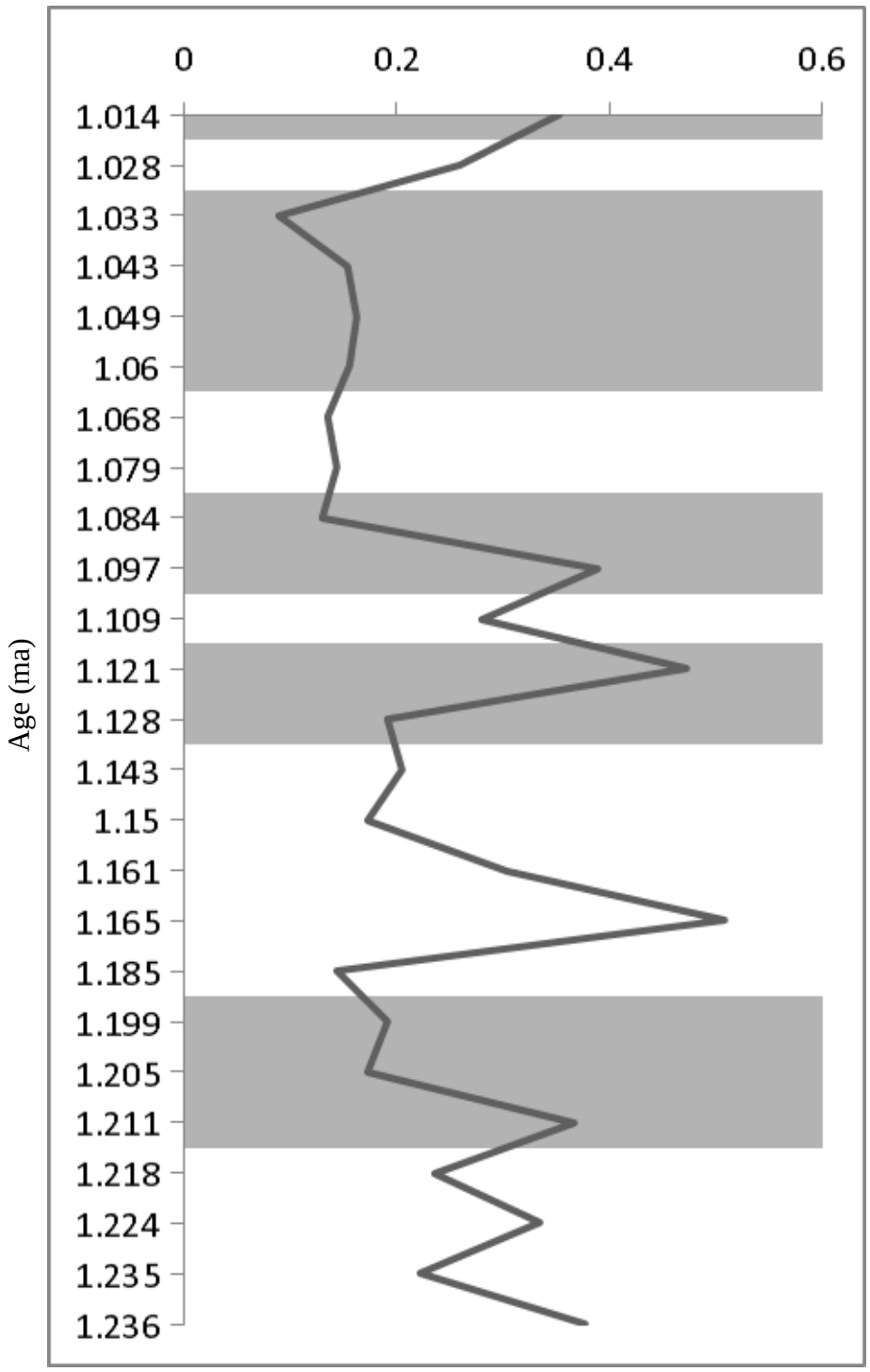

Figure 6: Illite/Quartz Intensity Ratio. Grey bands indicate glacials, white bands indicate interglacials.

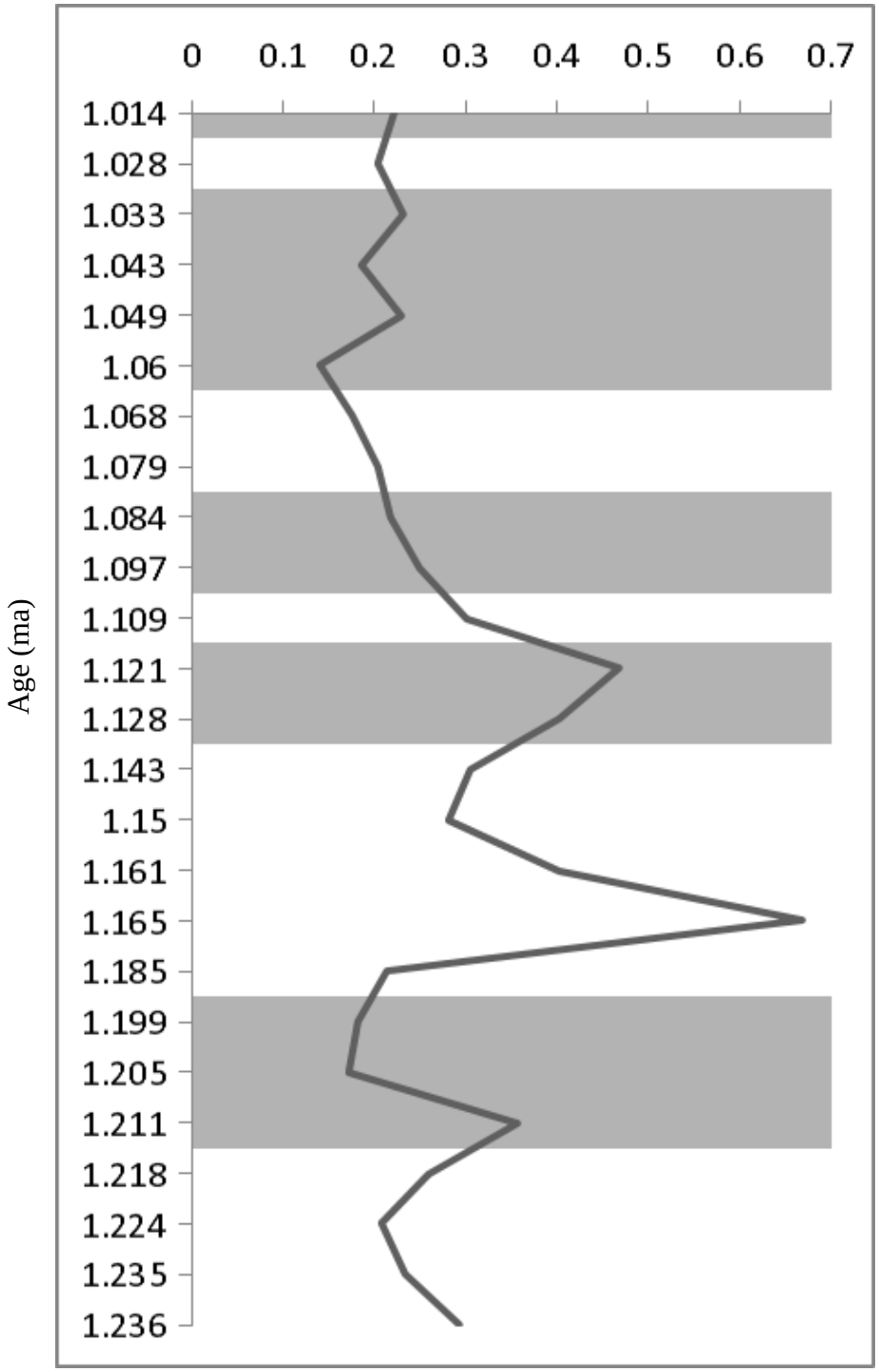

Figure 7: 7Å Clay/Quartz Intensity Ratio. Grey bands indicate glacials, white bands indicate interglacials.

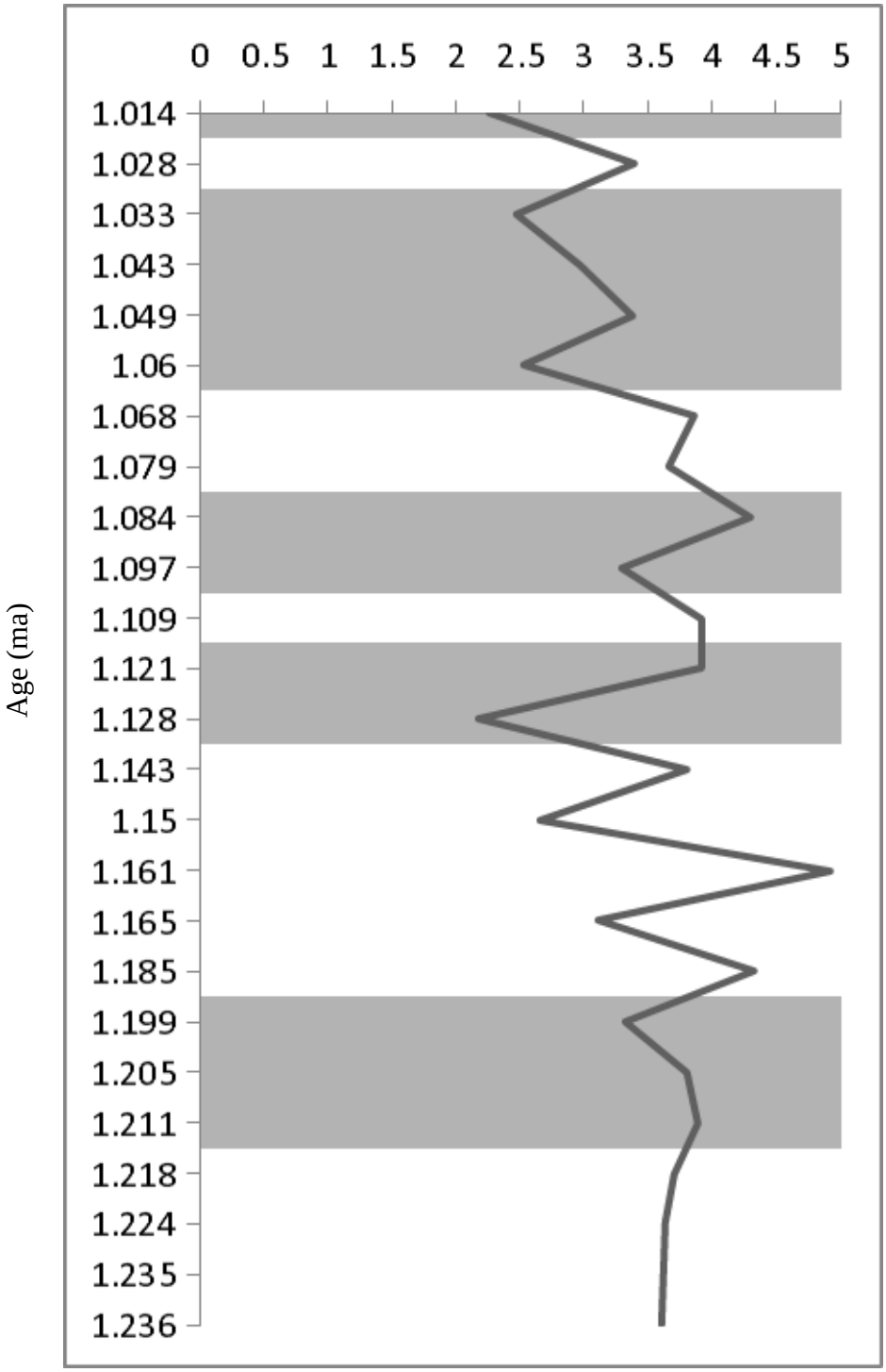

Figure 4: Calcite/Quartz Intensity Ratio. Grey bands indicate glacials, white bands indicate interglacials.

Table 4: Average Uncertainty of Mineral/Quartz Ratio

Mineral	Average Uncertainty of Ratio (%)
Quartz	4.38
Calcite/Quartz	4.48
Dolomite/Quartz	15.1
Illite/Quartz	26
7Å Clays/Quartz	14

Discussion

In general, none of the minerals identified showed a consistent pattern of peak intensity ratio changes relative to the glacial/interglacial stages. However, two pairs of minerals exhibited relatively similar abundance patterns. Quartz and dolomite abundances tend to trend together, as do illite and the 7Å clays. Calcite showed no particular pattern, and the halite was not consistently present. Halite will not be considered here, because seawater was used in the drilling fluid while obtaining the cores, and its presence is likely a result of evaporation of the drilling fluid.

These covarying patterns for quartz and dolomite and illite and the 7Å clays may be a result of similar grain sizes. Quartz and dolomite tend to be present as larger grain size particles, while illite and the 7Å clays tend to be smaller particles. In this case, then, the mineralogic changes may be a proxy for grain size variations, with grain size in turn an indicator of flow velocity. At higher velocities, smaller particles are washed away and larger particles remain in place, a process called winnowing. If this is true, then the presence of more quartz and dolomite indicates more winnowing, indicating a higher

velocity current. As a result, the times of higher current velocity may indicate times when the core of MOW was located at Site U1387.

Calcite shows no such pattern and much less variation over time, likely because it comes from both marine and terrestrial sources, which are affected by a wider range of environmental conditions.

The mineralogic data collected here do not support the original hypothesis that there should be some correlation between mineral abundances and glacial/interglacial cycles. This could be a result of a few factors. First is the fact that the Gulf of Cadiz contourite system is more complicated than originally proposed; factors other than the glacial/interglacial conditions affect the position of the MOW core and the composition of sediment being deposited. Current velocity at Site U1387 certainly will have an effect on sediment grain size and associated mineralogy, but velocity changes appear to respond to controls other than glacial/interglacial conditions. In addition, subtle changes in terrestrial weathering and sediment source areas may also affect this mineral record.

Secondly, there could be errors in the ages assigned to samples, resulting in samples not being assigned to the correct MIS. The ages for each sample are compared to well-established MIS boundaries, but the ages of the samples themselves could contain errors because those errors were calculated from the shipboard age-depth model. Any changes in sedimentation rate over the time period to which this rate was assigned could result in an incorrect age for a sample.

Future Work

To confirm the hypothesis that mineralogic associations reflect subtle changes in grain size, a detailed grain size analysis would need to be undertaken.

To help resolve the error associated with dating based on shipboard measurements, a necessary analysis would be oxygen isotope composition for the entire core to develop a more detailed age-depth model. This would allow for a better correlation with the glacial/interglacial cycle scale used in this study.

In addition, similar analyses of other sections of U1387 and comparison to these data would be useful for more confidence in relating mineralogy to glacial/interglacial cycles. Similar analyses of sediments of similar age but from different sites from Expedition 339 could give more insight on ocean current patterns, such as the vertical migration of the MOW core through time.

References

Expedition 339 Scientists, 2012a, Mediterranean Outflow Expedition 339: http://iodp.tamu.edu/scienceops/expeditions/mediterranean_outflow.html (accessed 4/3).

Expedition 339 Scientists, 2012b, Methods: http://publications.iodp.org/proceedings/339/102/102_.htm (accessed 4/3).

Hernández-Molina, F.J. et al, 2014: Onset of Mediterranean outflow into the North Atlantic: Science, v. 344, i.6189, p. 1245.

Hernández-Molina, F.J. et al, 2006: The contourite depositional system of the Gulf of Cadiz: A sedimentary model related to the bottom current activity of the Mediterranean outflow water and its interaction with the continental margin: Deep-Sea Research, v. II, i. 53, p. 1420–1463.

Lisiecki, L. E. and Raymo, M. E., A Pliocene-Pleistocene stack of 57 globally distributed benthic $d^{18}O$ records, Paleoceanography, 20, PA 1003, doi:10.1029/2004PA001071.

Appendix

Table 5: IODP Data of Samples

Hole	Core	Section	Meters Below Seafloor	Composite Depth (m)	Age (ma)
B	28	3	256.1	279.99	1.014
B	28	6	260.11	284	1.028
A	29	3	259.1	285.31	1.033
A	29	5	261.85	288.06	1.043
B	29	2	264.84	289.85	1.049
B	29	4	267.7	292.71	1.06
A	30	2	268	295.09	1.068
A	30	4	271	298.09	1.079
B	30	2	273.92	299.41	1.084
B	30	5	277.6	303.09	1.097
A	31	2	277.6	306.45	1.109
A	31	4	280.95	309.8	1.121
B	31	2	282.7	311.51	1.128
B	31	4	287	315.81	1.143
A	32	2	287.6	317.6	1.15
A	32	4	290.8	320.8	1.161
B	32	2	292.67	321.95	1.165
B	32	6	297.92	327.23	1.185
C	2	4	295.97	331.17	1.199
C	2	6	297.55	332.75	1.205
B	33	4	303.8	334.61	1.211
C	3	1	301.01	336.61	1.218
C	3	3	302.66	338.26	1.224
A	34	3	309	341.17	1.235
A	34	4	309.14	341.31	1.236